taining a satisfactory level of safety. Furthermore, a modeling approach such as that employed in this study suggests the capability for more detailed analysis of the controller's role in the air terminal system.

References

[1]Alexander, B. (chairman), "Report of Department of Transportation Air Traffic Advisory Committee," Vols. 1 and 2, Dept. of Transportation, Washington, D.C., Dec. 1969.

[2]Blumstein, A., "The Landing Capacity of a Runway," *Operations Research*, Vol. 7, No. 6, 1959, pp. 752–763.

[3]FAA, "The National Aviation System Plan, Ten Year Plan 1972–1981," (71-01686), March 1971, FAA, Washington, D.C.

[4]FAA, "The National Aviation System Policy Summary 1971," (7-10686), March 1971, FAA, Washington, D.C.

[5]Lister, S. F. and Raisbeck, G., "Approach to the Establishment of Practical Air Traffic Control Safety Goals," Contract No. FA70WA-2141, Little, Cambridge, Mass., May 1971.

[6]Raisbeck, G., Koopman, B. O., et al., "Air Traffic Control System Capacity," Contract No. DOT-FA70WA-2141, Little, Cambridge, Mass., Aug. 1970.

[7]Schriever, B. A. and Seifert, W. W., *Air Transportation 1975 and Beyond: A Systems Approach*, The MIT Press, Cambridge, Mass., 1968.

[8]Simpson, R., "Evaluation of Air Traffic Control Models and Simulations," Contract No. DOT-TSC-77, June 1971, MIT, Cambridge, Mass.

[9]Wilhelm, W. E., "Following Theory With Applications," Ph.D. dissertation, 1972, Virginia Polytechnic Inst. and State Univ., Blacksburg, Va.

JUNE 1973 J. AIRCRAFT VOL. 10, NO. 6

An Interactive Real Time Simulation for Scheduling and Monitoring of STOL Aircraft in the Terminal Area

John D. McLean* and Leonard Tobias*
NASA Ames Research Center, Moffett Field, Calif.

An interactive real time terminal area simulation has been developed to investigate performance requirements for STOL aircraft operations. Consideration is given to the interaction of the ground system with STOL aircraft using an onboard 4D guidance system. The simulation consists of four parts: 1) a scheduling algorithm which schedules conflict free arrival times at critical points; 2) a trajectory synthesizer which determines the reference trajectory from feeder fix to final approach; 3) a simultaneous simulation of all aircraft using 4D guidance along the synthesized reference trajectories; and 4) a graphic display used to present simulation results and interact manually with the simulation. This paper describes the simulation and presents results obtained to date.

Introduction

IN support of research on STOL terminal area operation, Ames is studying a promising new guidance concept, generally known as a "4D" guidance system.[1] The 4D guidance system synthesizes a curved three dimensional flight path and generates command inputs to fly along the path according to a time schedule specified by the ground system.

The 4D guidance system has the potential for enabling precise control of aircraft in a terminal area with low pilot workload provided accurate navigation data is available. An important problem arising in the use of a 4D guidance system is its interaction with the ground system. A ground system based on the time synchronized approach control concept considered by the FAA for terminal operation in the 1980's would generate sequencing, spacing, and time control commands which the aircraft must obey. The impact of such a ground concept on future STOL 4D guidance systems raises complex questions. These can only be investigated by a total system simulation that includes elements of both the airborne and the ground system.

This paper describes the current simulation and outlines the criteria used in developing it. First a description of the over-all system is given followed by a more detailed discussion of the individual components. Next the use of the simulation and display is described followed by a brief discussion of the results to date.

Presented as Paper 73-163 at the AIAA 11th Aerospace Sciences Meeting, Washington, D.C., January 10–12, 1973; submitted February 1, 1973; revision received April 12, 1973.

Index categories: Aircraft Navigation, Communication, and Traffic Control; Computer Technology and Computer Simulation Techniques; Navigation, Control and Guidance Theory.

*Research Scientist.

General Description of Simulation

This section gives an overview of the complete simulation showing the interaction of the various components. These components will be examined in more detail later.

The complete simulation is illustrated in block diagram form in Fig. 1. Once the system has been initialized the only function of the executive program is to provide the time control necessary for real-time operation. The aircraft scheduler accepts arriving aircraft generated at random time instants or from the keyboard associated with the graphic display. The mode of operation is determined by the operator. An aircraft can be one of three types; for example, CTOL, STOL, or VTOL. The type is also chosen randomly from a specified statistical distribution. The operator can also decide whether the arriving aircraft will be scheduled automatically or manually with computer aid. In either case, the scheduler transmits the set of waypoints describing the desired approach route to the trajectory synthesizer which develops a three-dimensional trajectory together with the maximum and minimum times required to travel between each pair of time-critical points.

The scheduler then selects appropriate times for the aircraft to pass through the time-critical points and calls upon the synthesizer to specify the trajectory in the form

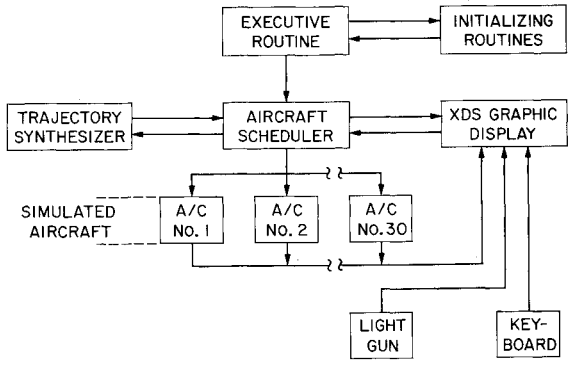

Fig. 1 Block diagram of complete simulation.

of a time sequence of commands. The scheduler then starts a simulated aircraft on the desired trajectory. The horizontal position, heading, and altitude of each aircraft as it progresses along the trajectory are displayed on a map of the terminal area. A second display, denoted the scheduling display, indicates the times that aircraft have been scheduled through the time critical points; this display is used by the operator for conflict free manual scheduling.

Since the efficient use of aircraft such as STOL and VTOL in urban areas will require very precise control of the trajectory it was felt necessary to include the effects of aircraft dynamics as well as navigation errors on the flight path. The dynamic model used will be described when the aircraft simulations are discussed later in the aircraft simulation section.

In the current version of the simulation, the number of aircraft in the terminal area is restricted to thirty during real-time operation. Since the primary interest of this simulation is to determine how V/STOL aircraft will perform in an advanced air-traffic environment and not to develop flow control models for large volumes of air traffic, the limitations on the number of aircraft is not a problem.

A sample situation display is shown in Fig. 2. This is a map of the San Francisco Bay Area showing a single runway located at San Francisco International Airport. The approach route from the north is for CTOL, while the one from the south is for STOL aircraft. The routes merge after which a single trajectory proceeds to the runway threshold. Runway and aircraft symbols are shown exaggerated in size. Note that the simulation is not limited to the configuration of trajectories shown in Fig. 2; however, for clarity of presentation, this configuration will consistently be used in the simulation description to follow. Moreover, it should not be assumed that landing CTOL and STOL on the same runway is advocated in this paper; rather, it should be understood that in some regions it may not be possible to construct a separate STOL runway and thus problems associated with intermixing of aircraft types should be anticipated by 4D guidance systems. Finally, it should be noted that, if utilization by CTOL and STOL of a single runway is necessary, merging the approach paths as late as possible is desirable since this will have the least detrimental effect on landing rate and will permit nominal trajectories to best fit aircraft capabilities.[3]

Next we will consider the individual components of the simulation in more detail.

Graphic Display and Aircraft Scheduler

The graphic display operates in either of two modes; the situation or "map" display shown in Fig. 2 and the scheduling or "window" display. The operation of the aircraft scheduler is very closely related to the window display

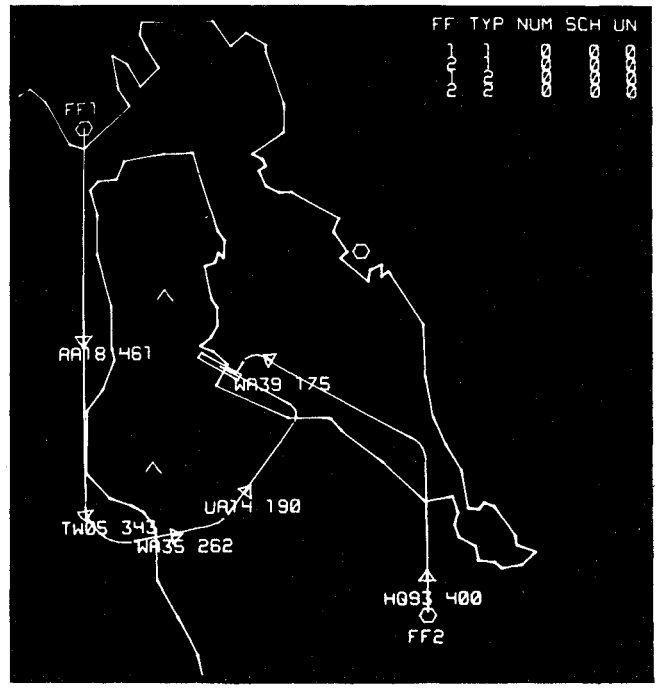

Fig. 2 Photograph of graphic display showing scenario used.

and these two parts of the simulation are best explained together.

Aircraft arrive in the terminal area shown in Fig. 2 according to a given random distribution; aircraft may also

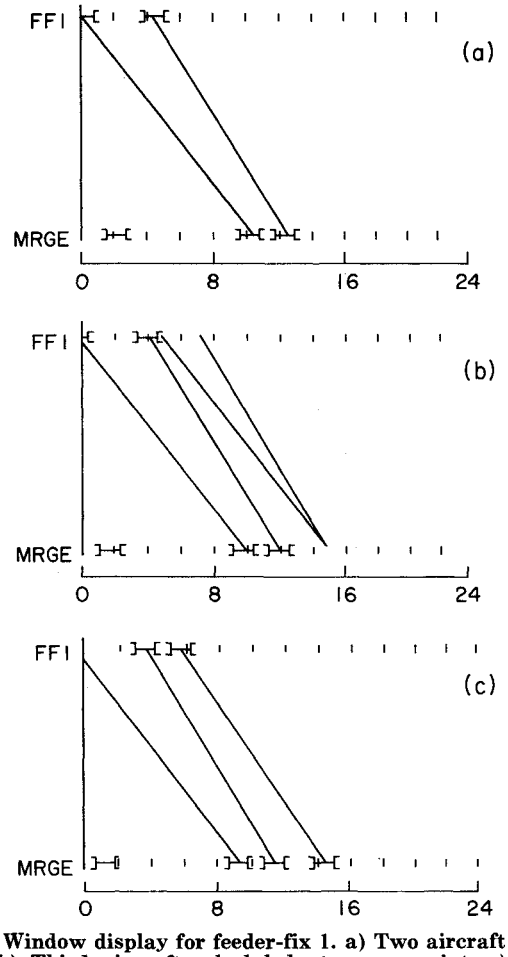

Fig. 3 Window display for feeder-fix 1. a) Two aircraft scheduled. b) Third aircraft scheduled at merge point. c) Third aircraft completely scheduled.

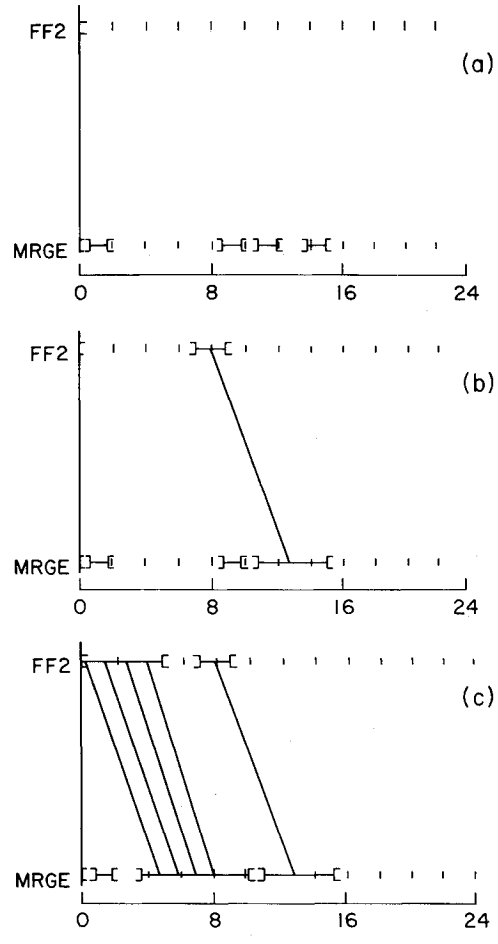

Fig. 4 Window display for feeder-fix 2. a) Merge-point times blocked out for feeder-fix 1. b) One aircraft scheduled from feeder-fix 2. c) Results of automatic scheduling.

be entered manually by the operator. A short time prior to arrival at the feeder-fix, the system is made aware of the impending arrival, and if possible the aircraft is scheduled without holding. If holding is necessary, it is assumed that it will take place at the feeder-fix. The aircraft symbol does not appear on the screen until its scheduled time of departure from the feeder-fix.

The chart in the upper right of Fig. 2 is a list of aircraft due to enter the system from each feeder-fix. In this figure the chart shows no aircraft waiting. The columns are, from left to right: 1) the feeder-fix number, 2) the type of aircraft, (The system is capable of handling multiple types of aircraft at each feeder-fix depending on the scenario chosen.), 3) the number of aircraft of that type waiting at the feeder-fix (aircraft which have notified the system of impending arrival or are holding at the feeder-fix), 4) the number of those aircraft which have been scheduled, and 5) the number of aircraft still to be scheduled.

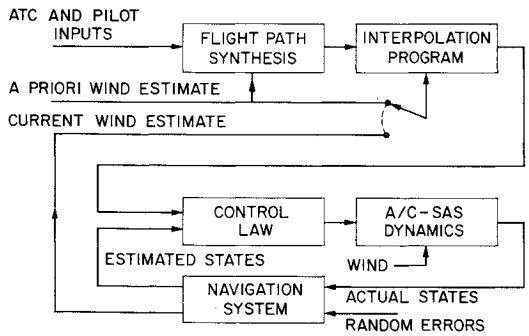

Fig. 5 Block diagram of single aircraft simulation.

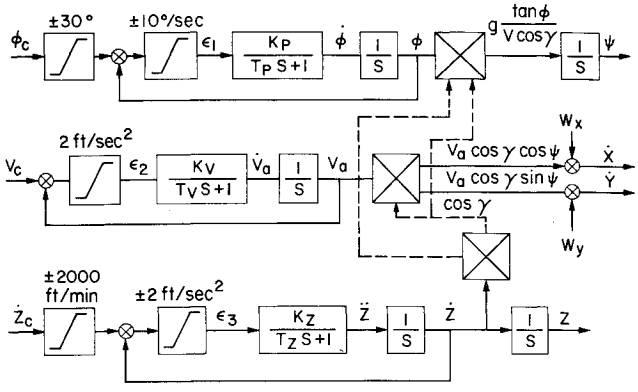

Fig. 6 Block diagram of aircraft-SAS dynamic model.

After an aircraft leaves the feeder-fix its position and heading are indicated by one of the triangular symbols. Associated with each aircraft symbol is an alphanumeric identification tag and the aircraft altitude in tens of feet. Only the two standard trajectories normally appear on the screen, but a nonstandard trajectory can be generated when an aircraft begins to follow it and removed when no longer needed.

The scheduling algorithm is designed to be used either as a fully automatic system or as an aid to a controller. In the automatic mode, as each aircraft enters the system, the algorithm assigns it a conflict-free time schedule for departure from the feeder-fix and passage through the merge point. The automatic procedure minimizes the landing time for the aircraft; the automated scheduling algorithm is described by Tobias.[2]

If aircraft are being scheduled manually, the operator uses function switches to select a feeder-fix and type which specify an unscheduled aircraft. (An error message is displayed if no aircraft of the type chosen is waiting to be scheduled at the feeder-fix.) A third function switch then causes the map display to be replaced by the appropriate window-display to be used for scheduling.

The window display for feeder-fix 1 is shown in Fig. 3a. The slanting lines indicate aircraft already scheduled. The horizontal coordinate of this display represents time from the present as shown on the bottom horizontal line. The present is indicated by zero and future time in hundreds of seconds from the present increases from left to right. The next horizontal line above the time scale represents time at the merge point and the third line is time at the feeder-fix. The vertical separation of these two lines can be thought of as the distance along the flight path from feeder-fix to merge point.

Now assume an aircraft is to be scheduled. First, the time for it to pass through the merge point is entered with the display keyboard and displayed on the screen for the controller's approval or disapproval. The controller enters a "1" from the keyboard to indicate approval and the display changes to that shown in Fig. 3b. The two rays originate at the time selected for passing through the merge point and terminate at the earliest and latest times at which the aircraft can leave the feeder-fix and arrive at the merge point at the desired time. When the controller selects and approves a time within this range, the display changes to that shown in Fig. 3c.

The ends of the slanting line indicate the time of departure from the feeder-fix and arrival at the merge point. The controller can use the light pen to approve of this schedule, in which case the aircraft is placed in a queue awaiting departure from the feeder-fix and the map display is returned. At any time during the scheduling process prior to this approval the controller can abort the process and start over.

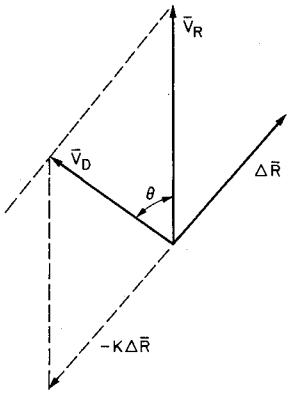

Fig. 7 Derivation of control law.

Note that a predetermined safety margin of time is blocked out on either side of a scheduled time. No other aircraft may be scheduled during the blocked out intervals, and schedules must be chosen so that the slant lines do not cross. (Crossing lines indicate an overtake situation.)

Now consider scheduling an aircraft at feeder-fix 2. The display for this case is shown in Fig. 4a. Note the times at the merge point which have been blocked out for the aircraft scheduled from feeder-fix 1. Figure 4b shows the result of manually scheduling an aircraft from feeder-fix 2 to arrive at the merge point between the last two aircraft scheduled from feeder-fix 1.

At the option of the controller, the scheduling can be done automatically. The results of scheduling four additional aircraft automatically is shown in Fig. 4c. Note that there are no gaps in the additional blocked out times and the slant lines are parallel because the scheduling algorithm chooses the earliest possible time at the merge point.

Aircraft Simulation

The simulation of each individual aircraft duplicates the single aircraft simulation shown in Fig. 5. The same trajectory synthesizer is used for all simulated aircraft, but it could be part of each onboard computation system.

Interpolation Program

The interpolation program takes the commands generated by the synthesizer and computes the reference state at each integration interval. This computation has been reduced to a set of simple algebraic and trigonometric equations by having the synthesizer command ground speed to be of the form $(v_0 + at)$. The change in ground speed during a turn caused by the presence of wind is accounted for by specifying the airspeeds at the beginning and end of the turn and using a constant acceleration to produce the net change in ground speed required. The estimated wind velocity used by the interpolation program may be either an a priori estimate used by the synthesizer

Table 1 Achieved separations under various unknown wind conditions

First type A/C to land	Followed by	Wind, knots	Minimum separation distance, ft
STOL	CTOL	0.	14531.
STOL	CTOL	15.	14147.
STOL	CTOL	30.	11122.
CTOL	STOL	0.	5711.
CTOL	STOL	15.	6135.
CTOL	STOL	30.	7451.

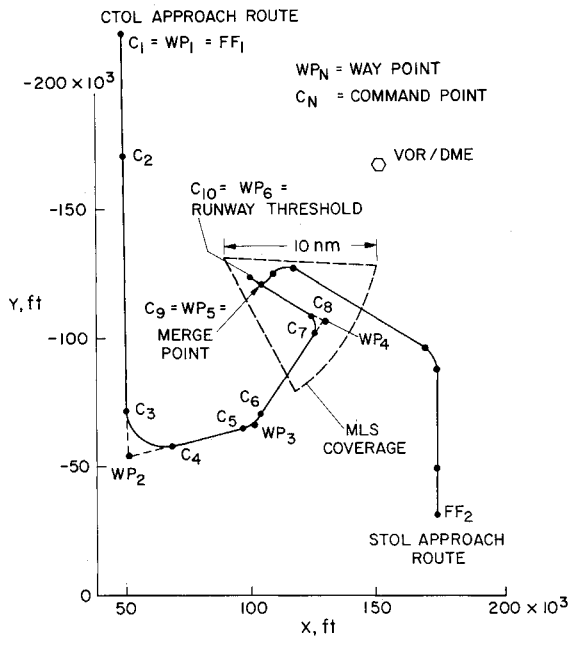

Fig. 8 Scenario used for combined STOL and CTOL operation.

or a current estimate obtained from the navigation system. Since the reference trajectory is specified in terms of ground velocity, the reference velocity vector, $\bar{V}_R$, relative to the air mass will differ depending on which wind estimate is used. These velocities will be referred to as the a priori and current values of $\bar{V}_R$, respectively.

Navigation System

The navigation system generates appropriate errors which are added to the actual states to give the estimated state used in the control law. Two types of radio aids are considered; VOR/DME used in conjunction with a baro-altimeter or the microwave landing system (MLS), configuration K.[4] The radio aid and baro-altimeter data are combined with accelerometer signals through a comple-

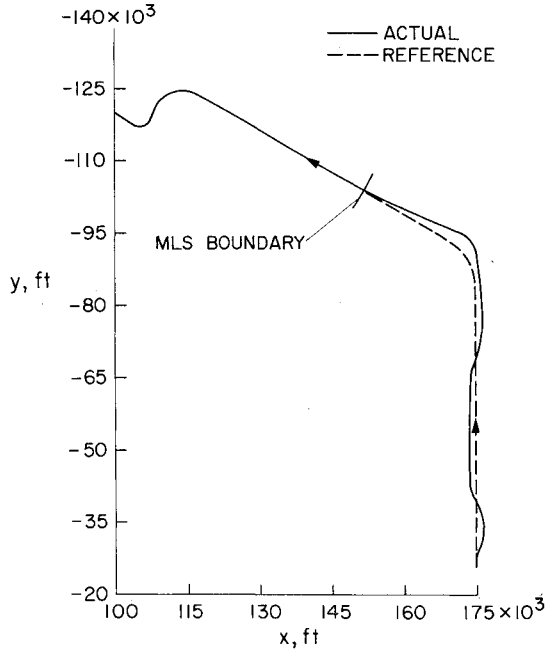

Fig. 9 Actual and reference trajectories in presence of navigation errors.

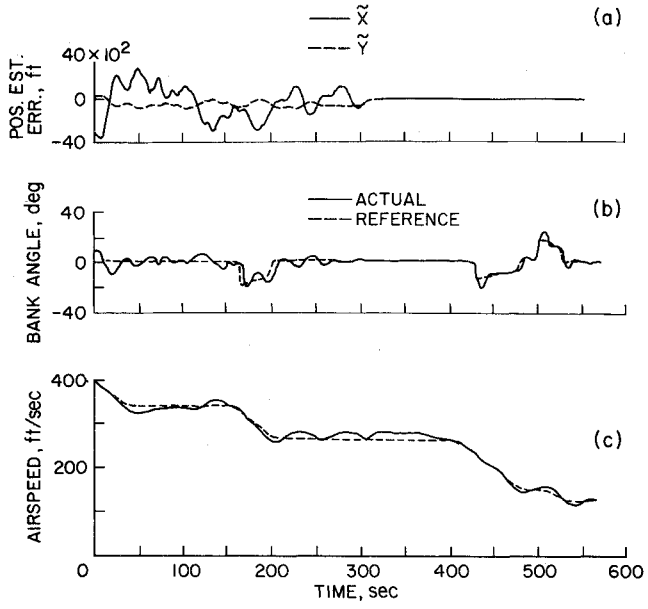

Fig. 10 Time histories of estimation errors and control actions. a) Position estimation errors. b) Bank angle. c) Airspeed.

mentary filter. Dead reckoning computations are also provided for regions where VOR/DME and MLS are not usable, such as at elevation angles of more than 30° above the VOR transmitter.

The error model for VOR/DME is given by Johansen[5] and contains a velocity dependent term. The errors in angular and range measurements for MLS are assumed to consist of a bias plus white noise, and biases were also considered to be satisfactory approximations for errors in heading and true airspeed. The baro-altimeter errors are approximated by a randomly chosen bias multiplied by airspeed.

Aircraft Dynamics

The aircraft and SAS dynamics are lumped together in a simplified model chosen to represent the closed loop airplane-autopilot system. This model is shown in block diagram form in Fig 6. Saturation limits are provided on bank angle command, roll rate, vertical and longitudinal acceleration, and climb and descent rate. Also, the roll rate and linear accelerations are restricted to finite rates of change by the time lags. This model was obtained by fitting transient responses from a large detailed simulation of a DC-8 with a digital autopilot.[6] The simplified model was considered satisfactory since its flight path corresponded closely to that of the detailed simulation when the same sequence of commands, necessary to follow a complex trajectory, was used with each system with no corrective feedback.

Integration of the equations of motion is accomplished using the following simplified method. (Note that if an additional integration is added to the velocity channel then all three channels have the same form.) Taking the lateral channel as an example we assume that ϵ_1 is constant during each integration interval and solve for the increments in the variables at the end of the interval. The equations for these increments, denoted by Δ, are

$$\Delta\dot{\phi}(t_0 + h) = (k_p\epsilon_1 - \dot{\phi}_0)(1 - e^{-h/\tau_p})$$

$$\Delta\phi(t_0 + h) = k_p\epsilon_1 h - \tau_p\Delta\dot{\phi}$$

$$\Delta\beta \triangleq \int_{t_0}^{t_0+h} \phi(t)dt = k_p\epsilon_1\frac{h^2}{2} - \tau_p\Delta\phi + h(\phi_0 + \tau_p\dot{\phi}_0) \quad (1)$$

where h is the integration step size and the subscript 0 indicates values at the beginning of the interval.

The change in heading, $\Delta\psi$, requires some extra computation since

$$\dot{\psi} = \frac{(g - \ddot{Z})}{V_a \cos\gamma}\tan\phi \quad (2)$$

which can be written

$$\dot{\psi} = \frac{(g - \ddot{Z}_0 - \Delta\ddot{Z})\tan(\phi_0 + \Delta\phi)}{(V_0 + \Delta V_a)\cos(\gamma_0 + \Delta\gamma)} \quad (3)$$

It can be shown that $\Delta\ddot{Z}$, ΔV_a, and $\Delta\gamma$ may be neglected so that

$$\dot{\psi} \approx \frac{(g - \ddot{Z}_0)}{(V_0 \cos\gamma_0)}\tan(\phi_0 + \Delta\phi) \quad (4)$$

which can be approximated by

$$\dot{\psi} \approx \frac{(g - \ddot{Z}_0)}{(V_0 \cos\gamma_0)}(\tan\phi_0 + \Delta\phi \sec^2\phi_0) \quad (5)$$

Since $\Delta\phi = \phi(t) - \phi_0$

$$\Delta\psi = \frac{(g - \ddot{Z}_0)}{(V_0 \cos\gamma_0)}[\Delta\beta \sec^2\phi_0 + h(\tan\phi_0 - \phi_0 \sec^2\phi_0)] \quad (6)$$

Equations similar to Eq. (1) are used for the other two channels to get ΔV_a and ΔZ. In order to obtain ΔX and ΔY we assume that the motion relative to the air mass in the horizontal plane is either straight or circular, and note that

$$\Delta S \triangleq \int_{t_0}^{t_0+h} V_a dt$$

is the total distance traveled relative to the wind during one integration interval. Then it can be shown that

$$\Delta X = C\cos\psi_0 + hW_x$$

$$\Delta Y = C\sin\psi_0 + hW_y \quad (7)$$

where hW_x and hW_y are the changes in position caused by the wind and the quantity

$$C = [\Delta S^2 - \Delta Z^2]^{1/2} \quad (8)$$

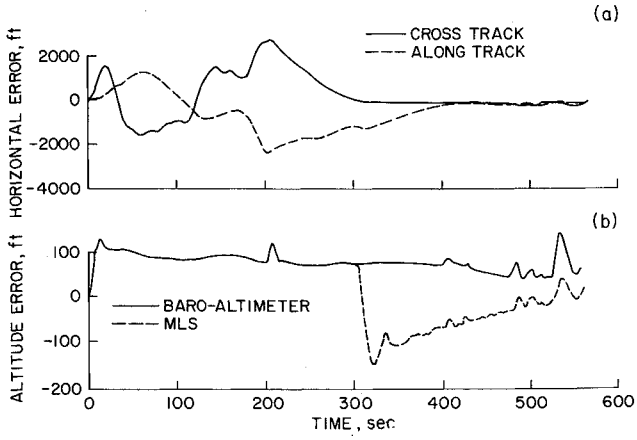

Fig. 11 Tracking errors. a) Errors in horizontal plane. b) Altitude errors.

is the chord length of the arc which is the projection of ΔS onto the X-Y plane.

Control Law

The control law is derived with the aid of Fig. 7. Here $\bar{V}_R$ is the reference velocity and $\Delta\bar{R}$ is the position error vector. The desired velocity vector $\bar{V}_D$ is chosen such that the difference between $\bar{V}_D$ and $\bar{V}_R$ will null $\Delta\bar{R}$; that is

$$\bar{V}_D = \bar{V}_R - K\Delta\bar{R} \tag{9}$$

Note that $\bar{V}_D$ and $\bar{V}_R$ may be regarded as velocities relative to the air mass since the wind velocity will appear on both sides of the equation if it is accounted for. The value of K is nominally constant; however for large errors it is reduced so that $|\bar{V}_D|$ will be within the allowable bounds on airspeed, and so that the difference, θ, between reference and commanded headings will not exceed 90°.

The velocity $\bar{V}_R$ is computed by subtracting the components of the estimated wind velocity from the reference ground velocity. Thus if the a priori wind estimate used in the synthesizer program is incorrect, a "correct" value for $\bar{V}_R$ may still be obtained if the current wind estimate from the navigation system is accurate. However, with large differences between the a priori and current wind estimates, this approach may call for airspeeds which exceed the allowable limits. in that case a complete recomputation of the reference trajectory by the synthesizer is required.

The vector equation for $\bar{V}_D$ is translated into commands for the auto-pilot-autothrottle system by means of the equations of motion to give

$$\psi_D = \tan^{-1}\left(\frac{V_y - K\Delta y}{V_x - K\Delta x}\right) \tag{10}$$

$$V_D \approx V_D \cos\gamma = [(V_y - K\Delta y)^2 + (V_x - K\Delta x)^2]^{1/2}$$

$$\dot{Z}_D = -K\Delta Z \tag{11}$$

These quantities are the heading, airspeed, and change in altitude necessary to null the errors between the actual and reference trajectories. The commands to the aircraft consist of these quantities together with the appropriate derivatives necessary to provide zero steady state position errors for constant reference heading rate, altitude rate, or rate of change of airspeed. Note that the vertical channel is essentially uncoupled from the other two, and the value of K in Eq. (10) may be different from that in Eq. (11).

Since the control variable in the lateral channel is ϕ instead of ψ a heading-angle feedback must be added. The heading error is multiplied by V_a to compensate for the division by V_a in the computation of $\dot{\psi}$. Also, some variation in the gain, K_ϕ, of the autopilot bank-angle feedback has been allowed in order to improve the speed of response. The resulting commands to the autopilot are

$$\begin{aligned} \phi_c &= K_\psi V_a(\psi_D - \psi) + K_\phi \phi_D \\ V_c &= V_D + \dot{V}_D/K_v \\ \dot{Z}_c &= -K\Delta Z + \dot{Z}_R \end{aligned} \tag{12}$$

where the subscript R refers to the reference states.

The quantity ϕ_D is obtained from the equation

$$\dot{\psi}_D = \frac{g\tan\phi_D}{V_D} \tag{13}$$

using the derivative of the expression for ψ_D in Eq. (10). The result is

$$\begin{aligned} \phi_D = \tan^{-1}\{\frac{1}{g}[&(\dot{V}_y - K\Delta\dot{y})\cos\psi_D \\ &- (\dot{V}_x - K\Delta\dot{x})\sin\psi_D]\} \end{aligned} \tag{14}$$

while differentiating the expression for V_D gives

$$\dot{V}_D = (\dot{V}_x - K\Delta\dot{x})\cos\psi_D + (\dot{V}_y - K\Delta\dot{y})\sin\psi_D \tag{15}$$

For sufficiently small values of ΔX and ΔY these commands are equivalent to the control law given in Ref. 1 and the same stability analysis methods can be used.

Trajectory Synthesizer

The trajectory synthesizer program is described in detail by Erzberger and Pecsvaradi,[1] and will be discussed only briefly here. Consider the CTOL approach trajectory shown in Fig. 8. It is specified to the synthesizer by means of the Cartesian coordinates of the waypoints WP_1, WP_2 ... and the allowable airspeed ranges between waypoints. The horizontal trajectory and altitude profile are determined together with the maximum and minimum times to travel between time-critical waypoints. In this case, the time to depart the feeder-fix and the time to pass through the merge point are the control times.

The aircraft's onboard computer is then used to generate a sequence of command points C_1, C_2.... The command points as illustrated in Fig. 8 are at the start of new segments of the flight path, which consists of straight line segments and circular arcs. Each command point indicates a change in heading rate, flight-path angle, airspeed rate or in some combination of these quantities. These commands are used by the interpolator as discussed earlier to generate the reference states as time progresses.

Results to Date

A combined STOL and CTOL operation was investigated using the scenario depicted in Fig. 8. The VOR/DME indicated in the figure was used for navigation, and a conservative assumption for MLS coverage was assumed as indicated. The commanded airspeed was arbitrarily restricted to be within 10% of the a priori reference value. The same dynamics were used for the STOL aircraft as for the CTOL except, of course, for the speed and glide slope capabilities. Examination of transient responses calculated for a preliminary version of a STOL SAS and speed control system for the C-8A aircraft showed this to be a reasonable assumption. It should be pointed out that the trajectories used in this study were chosen solely for the purpose of investigating STOL interactions with proposed advanced ATC environments. They are not suggested as actual approach routes in any terminal area.

The effects of wind and of mixed speed classes using the same runway on scheduled minimum separation distances were investigated using this configuration. The runway threshold point is a time-controlled point. A minimum time separation of 60 sec was specified for any two consecutive aircraft; CTOL final approach speed was 120 knots, while STOL was 80 knots. Table I shows the minimum separation distances that were actually obtained in the simulation with winds of various magnitudes in opposite direction to that of aircraft landing. (Note that these are *unknown* winds.) Clearly, if a minimum separation distance between aircraft of two nautical miles is to be maintained the time separation to be specified at time control points is strongly dependent on the sequence of aircraft types, the wind conditions, and the path geometry. A more detailed study of this interaction is underway.

The next figures show the effects of navigation errors for one sample trajectory. The aircraft was initially on the

reference trajectory and there was no wind. Figure 9 shows the superimposed X-Y plots of the actual and reference trajectories. Note the large deviations from the reference trajectory during the first portion of the trajectory, while in the MLS region the errors decrease to fairly small values. In the first straight-line portion of the trajectory the aircraft is headed almost directly towards the VOR station so that the cross track errors are due mostly to VOR angular error.

Figure 10 shows time histories of the errors in estimating position and the resulting control actions. Note the sudden reduction in estimation errors (Fig. 10a) at about 300 sec; this being the point where the aircraft enters the region where MLS is available. During VOR/DME operation the X component, $\tilde{x}$, of the position error decreases with range to the transmitter. On the other hand, $\tilde{y}$ is smaller and has a frequency content characteristic of the DME error, which consists of a bias plus random errors with a long correlation time. (Electronic noise, being of relatively high frequency, was omitted from the simulation since it could be effectively removed by filtering.)

Early in the trajectory, position estimation errors exceed 4000 ft. However, as the distance to the VOR/DME transmitter is reduced, the position measurement errors decrease to about 1000 ft just before the MLS coverage is entered. The corresponding velocity errors, and therefore the current wind estimate, are so large as to be useless for control.

These large estimation errors required some revisions of the navigation system and control law while using VOR/DME in order to provide reasonable tracking accuracy without excessive control activity. This was accomplished by varying the gain [K in Eq. (9)] on the position error feedback inversely with range to the VOR transmitter and by estimating velocity solely from air data measurements during VOR/DME operation. Figures 10b and 10c show the resulting control actions used by the aircraft in trying to follow the reference trajectory. During the first part of the trajectory, where VOR/DME is used, the roll angle oscillates about the reference value with an amplitude of a few degrees and a fairly long period. Additional study is needed to determine whether the bank angle activity is satisfactory from the standpoint of passenger comfort. There is also some variation in airspeed due to navigation errors but it is felt that the required throttle activity would be acceptable. After entering the MLS region the deviations from the reference roll angle are negligible except during transients caused by commanded turns and the deviations of airspeed from the reference value are considerably smaller.

The tracking errors are plotted in Fig. 11. The horizontal error, referred to in an along track and cross track reference system, is shown in Fig. 11a. These errors decrease rather slowly after entering the MLS region because of the limited amount of speed control available and because there is a bias error in the measured airspeed used for the velocity control feedback. This bias error results in a small steady-state error in the final portion of the trajectory since it is equivalent to an unknown wind along the flight path.

Figure 11b shows two time histories of altitude deviations from the reference trajectory. One is the result of using baro-altimeter measurements over the entire trajectory while the other uses MLS for altitude determination in the region where it is valid. The errors are smaller in the case where MLS is used, but an undesirable high frequency component is present. This could undoubtedly be reduced by improvements in the vertical channel of the complementary filter.

These results indicate that precise spacing using 4D guidance can be achieved only with the aid of a navigation system of comparable accuracy to MLS. In addition, the data just presented indicates the need for modifications to the navigation system and the control law during the VOR/DME mode. These revisions allow delivery of the aircraft into the high-accuracy navigation region with sufficiently small deviations from the reference trajectory while avoiding excessive bank angle and throttle activity.

Concluding Remarks

An interactive real time simulation has been described which consists of a scheduling algorithm which can be used in either an automatic or controller assisted mode; a trajectory synthesizer which determines the reference trajectory from feeder fix to final approach; an aircraft system simulation which includes the navigation system; aircraft and autopilot dynamics and control law; and a graphic display used to present simulation results and to interact manually with the simulation. Initial results have been presented on how the combined operation of STOL and CTOL aircraft using the time synchronized approach control concepts anticipated by the FAA for the 1980 time period would affect STOL performance requirements. Two effects on spacing of aircraft were investigated. First the effects of wind and of mixed speed classes using the same runway on minimum spacing were described. Second, the navigation aids needed to achieve precise spacing for an operating 4D guidance system were discussed.

Continued research is planned in the above areas as well as investigations of STOL requirements for missed approach and collision avoidance maneuvers. A data link to a pilot operated simulation will permit investigation of pilot tasks in an automated 4D environment.

References

[1] Erzberger, H. and Pecsvaradi, T., "4-D Guidance System Design with Application to STOL Air Traffic Control," *Proceedings of the 1972 Joint Automatic Control Conference of the American Automatic Control Council,* Stanford Univ., Stanford, Calif., Aug., 1972.

[2] Tobias, L., "Automated Aircraft Scheduling Methods in the Near Terminal Area," *Journal of Aircraft,* Vol. 9, No. 8, Aug. 1972, pp. 520–524.

[3] Straeter, T. A., Park, S. K., and Hogge, J. E., "Application of Optimization Techniques to Near Terminal Area Sequencing and Flow Control," *Proceedings of the 1972 Joint Automatic Control Conference of the American Automatic Control Council,* Stanford Univ., Stanford, Calif., Aug. 1972.

[4] A New Guidance System for Approach and Landing," RTCA Doc. DO-148, Dec. 18, 1970, Radio Technical Commission for Aeronautics, Washington D.C.

[5] Johansen, H., "A Survey of General Coverage NAVAIDS for V/STOL Aircraft," CR1588, May 1970, NASA.

[6] Osder, S., Neuman, F., and Foster, J., "Digital Autopilots: Design Considerations and Simulator Evaluations," TM X-62,094, Oct. 1971, NASA.